



# The phase transitions in selective laser-melted 18-Ni (300-grade) maraging steel

Mariusz Król<sup>1</sup> · Przemysław Snopiński<sup>1</sup> · Adam Czech<sup>2</sup>

Received: 16 August 2019 / Accepted: 10 January 2020 / Published online: 21 January 2020  
© The Author(s) 2020

## Abstract

Dilatometric studies in 18-Ni steel components fabricated by selective laser melting technique were carried out to determine the influence of heating rate on transitions occurring during the heating cycle. SLM components have been examined in controlled heating and cooling cycles. For analysis, heating of the analysed materials was carried out at heating rates of 10, 15, 20, 30 and 60 °C min<sup>-1</sup>. During the heating process, two solid-state reactions were identified—i.e. precipitation of intermetallic phases and the reversion of martensite to austenite. A simplified procedure based on the Kissinger equation was used to determine the activation energy of individual reactions. For precipitation of intermetallic phases, the activation energy was estimated 301 kJ mol<sup>-1</sup>, while the martensite to austenite reversion was determined at the activation energy 478 kJ mol<sup>-1</sup>.

**Keywords** Maraging steels · Precipitation · Martensite reversion · Phase transitions

## Introduction

Maraging steel contains an extremely low amount of carbon (0.03% maximum) and a high amount of nickel (17–19%) together with lesser amounts of cobalt (8–12%), molybdenum (3–5%), titanium (0.2–1.8%) and aluminium (0.1–0.15%). This type of iron alloys belongs to the group of materials that are characterised as a martensitic crystal structure and strengthened by ageing heat treatment at approximately 500 °C, hence the name ‘maraging’. This ultra-low-carbon alloy has very high-strength high-toughness alloy that gain their exceptional mechanical properties derived from precipitation of intermetallic compounds and a martensitic matrix. The martensitic microstructure is not obtained by a high carbon content but by addition of nickel as one of the main element in chemical composition. The ultra-high-strength maraging steel is attracted by material engineers and structural designers of aerospace, machining

areas, nuclear and defence industries. They are classified into M200, M250, M300 and M350 grades according to their 0.2% proof stress or yield strength levels, namely 200, 250, 300 and 350 ksi [1, 2].

The maraging steels are usually subjected to heat treatment—hardening and then ageing at a temperature of 450–510 °C, which causes a significant increase in hardness and strength in the effect of precipitations [3, 4] of  $\gamma$ -Ni<sub>3</sub>Mo,  $\eta$ -Ni<sub>3</sub>Ti, Fe<sub>2</sub>Mo,  $\sigma$ -FeMo,  $\mu$ -Fe<sub>7</sub>Mo<sub>6</sub>, FeTi, Fe<sub>2</sub>Ti [4–6]. This causes nickel enrichment in the matrix, stabilising the austenite and reducing the initial temperature of the martensite-to-austenite transitions or reversion [7–12]. It should be noted that during these transitions, both shear and diffusion mechanisms can occur simultaneously [8, 13]. These mechanisms may depend on the heating rate, as was stated by Carvalho et al. and Reis et al. [14, 15].

The transitions kinetics of the reaction in solid state in a component may be diagnosed by quantifying the variation in physical properties such as hardness, dilation, electrical resistivity or enthalpy as a function of reaction temperature and time. One of the methods that provide precise information about transitions in solid state during heating and cooling cycles is dilatometry [16–23]. This technique is a very sensitive and appropriate method for examining phase transformations, which revealed its strengths on measurements of a wide range of steels, such as maraging steels and low-carbon steels. The dilatometer is used to precisely measure

✉ Mariusz Król  
mariusz.krol@polsl.pl

<sup>1</sup> Department of Engineering Materials and Biomaterials, Faculty of Mechanical Engineering, Silesian University of Technology, Konarskiego 18a St, 44-100 Gliwice, Poland

<sup>2</sup> Department of Lightweight Structures and Polymer Technology, Chemnitz University of Technology, Chemnitz, Germany

dimensional changes of a component caused by changes in the thermal environment under extreme conditions of controlled heating and cooling. Solid or hollow samples are inductively warming up to a temperature plateau and are then continuously cooled with different rates (linear or exponential). Common applications embrace thermal expansion, annealing studies, determination of phase transformations and the glass transition, softening points, kinetics studies, development of phase diagrams, including the determination of sintering temperature, sintering step and rate-controlled sintering. The phase transitions taking place in the continuous cooling process or the isothermal plateau is indicated by the determined difference of length [14, 15, 18, 19, 22–25].

The absence of carbon in the chemical composition of maraging steel affects good on weldability, and therefore makes these alloys favoured candidates for additive manufacturing techniques, such as selective laser melting (SLM). In this technique, a focused laser beam is used to spot on the powder beds and successive melting of the powder layer with bonding to existing layers, which result is the manufacturing of 3D model. SLM technology has many advantages over other parts manufacturing technologies, including considerable material utilisation, comfortable product design, good part and production flexibility and functional properties of the obtained models using the appropriate production parameters [26–29].

The present work was carried out on components from maraging 300 steel fabricated by selective laser melting technique using a very sensitive computer-controlled BAHR DIL805 A/D dilatometer to study the effect of heating rate on both the precipitation and the martensite-to-austenite transitions, as well as to analyse the activation energies of these phase transitions during the heating cycle.

## Experimental procedure

In this work, 18-Ni 300 steel supplied by BÖHLER as a gas-atomised powder in size 15–45  $\mu\text{m}$  and spherical shape was used to manufacture samples by selective laser melting technique. The chemical composition of the applied powder is given in Table 1. Preparation of the components by SLM technique, the RENISHAW AM125 AM system with a Ytterbium (Yb) fibre laser of maximum laser power (200 W), scan speed (2000  $\text{mm s}^{-1}$ ) and wavelength (1074 nm) were used. The samples were produced on the mild steel substrate without preheating at an oxygen level

below 500 ppm. Components were fabricated applying a meander scanning strategy which consisted of changing the scan direction of each subsequent layer by  $67^\circ$ .

For dilatometric measurements, cylindrical samples 4 mm in diameter and 10 mm long were manufactured. The heating and cooling process was carried out in the quenching BAHR DIL805 A/D dilatometer linked to the personal computer with software for data acquisition system was used for the experiment, which consisted of heating the samples in a low vacuum of  $10^{-4}$  mbar to 900  $^\circ\text{C}$  at different heating rates, from 10 to 60  $^\circ\text{C min}^{-1}$ . A calibrated S-type thermocouple centrally spot-welded to the surface was used for temperature measurement. All of the samples were held between two  $\text{Al}_2\text{O}_3$  push rods, with one of the rods fastened, and the other one connected to the linear variable displacement transducer (LVDT).

Length increase ( $\Delta L$ ) and temperature ( $T$ ) changes were captured during heating for each heating rate. The Savitzky–Golay method was used as a signal smoothing processing of the differential data.

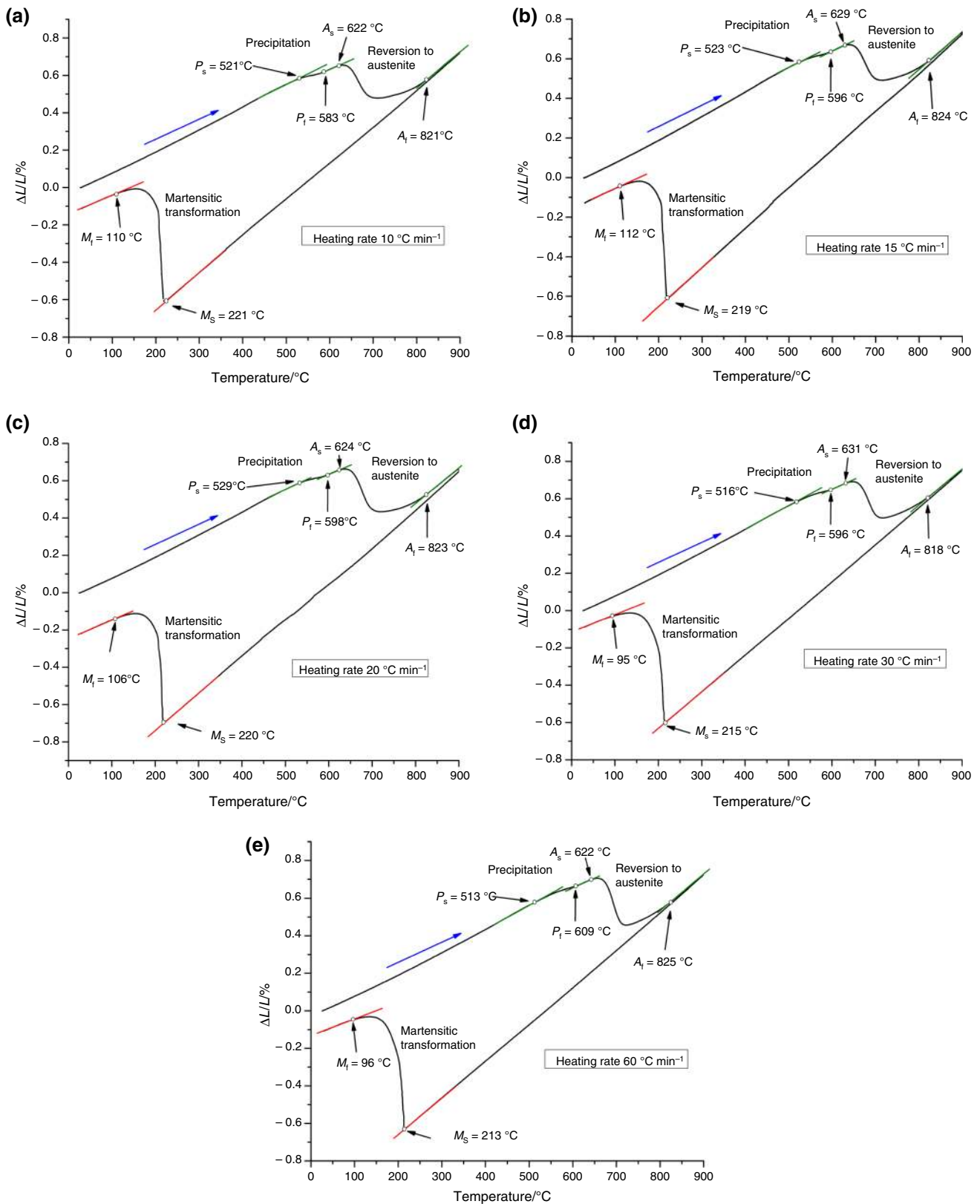
## Results and discussion

Figure 1 presents typical dilatometric curves of components fabricated in the SLM technique in as-built condition for total heating to 900  $^\circ\text{C}$  and cooling cycles, inflections from tangents to the curve expressing the phase transitions temperatures. Changes in example length,  $\Delta L$ , with regard to initial length,  $l_0$ , are graphed as a function of temperature. Through the heating and cooling periods, three-phase transitions in analysed maraging steel can be found and recognised. The first changes in angle slope of the line from the primary straight line portion are related to the development of the main strengthening precipitates, namely the  $\text{Ni}_3\text{Ti}$  and  $\text{Ni}_3\text{Mo}$  phases followed by the  $\text{Fe}_2\text{Mo}$  or  $\text{Fe}_7\text{Mo}_6$  phases. The second variation at higher temperature is affected by the austenite reversion  $\alpha' \rightarrow \gamma$  transition by shear and to the dissolution of precipitates [24]. The third deviation found out during measurement is a martensitic transition that occurs through the continuous cooling cycle. All of the phase transitions temperatures are given in Table 2.

Generally, investigated material is defined by uniform expansion continues till 513–529  $^\circ\text{C}$ , when a small shrinkage takes place, symbolising the beginning of precipitation at this temperature ( $P_s$ ). In the next step, a small quantity of linear expansion takes place with increasing temperature to

**Table 1** Chemical composition of the maraging steel 18-Ni 300 powder declared by the producer

Element/mass%	Ni	Mo	Co	Ti	Cr	C	Si	Mn
18-Ni 300	17–19	4.5–5.2	8.5–10	0.6–1.2	<0.25	<0.03	<0.1	<0.15



**Fig. 1** Relative sample length change,  $\Delta L/L_0$ , samples at **a** 10 °C min<sup>-1</sup>; **b** 15 °C min<sup>-1</sup>; **c** 20 °C min<sup>-1</sup>; **d** 30 °C min<sup>-1</sup>; **e** 60 °C min<sup>-1</sup> SLM samples as a function of temperature

**Table 2** Phase transition temperatures of analysed maraging steel with different heating rates

Heating rate/ $^{\circ}\text{C min}^{-1}$	$P_s$ -precipitations start/ $^{\circ}\text{C}$	$P_f$ -precipitations finish/ $^{\circ}\text{C}$	$A_s$ -austenite transition start/ $^{\circ}\text{C}$	$A_f$ -austenite transition finish/ $^{\circ}\text{C}$	$M_s$ -martensite start/ $^{\circ}\text{C}$	$M_f$ -martensite finish/ $^{\circ}\text{C}$
10	521	583	622	821	221	110
15	523	596	629	824	219	112
20	529	598	624	823	220	106
30	516	596	631	818	215	95
60	513	609	642	825	213	96

583–609  $^{\circ}\text{C}$  ( $P_f$ ), where precipitation ends. While the temperature is increased to 622–642  $^{\circ}\text{C}$ , a massive shrinkage arises in the dilatometry line, which can be identified as the beginning of the austenite formation ( $A_s$ ). At 818–825  $^{\circ}\text{C}$ , the curve reassumes linear expansion; consequently, the austenite transformation finishes ( $A_f$ ). The total solution is reached by heating continuously to 900  $^{\circ}\text{C}$  and isothermal holding at that temperature for 30 min. Through cooling cycle to ambient temperature, extreme expansion at approximately 213–221  $^{\circ}\text{C}$  can be observed, thanks to the rapid start and the fast transition from austenite to martensite, agreeing to the temperature of martensite start ( $M_s$ ). Martensite formation results in expansion because the structure is changed from FCC to BCT through polymorphic transformation. The transition to the martensite finishes ( $M_f$ ) at approx. 95–129  $^{\circ}\text{C}$ . Therefore, a single-phase microstructure should characterise maraging 300 steel upon cooling to an ambient temperature that is martensite.

Based on captured results, it can be stated that the transition temperatures are dependent on heating rate as Kapoor et al. [13] revealed that the reversion process are taking place by diffusion or by shear, and it depends on the heating rates. Increase in the heating rate causes increase in the transition temperatures. That aspect may be interpreted with reference to the diffusional character of the reaction, which depends on the temperature and the time at that temperature [3]. As the heating rate is raised, the time at that particular temperature of the mechanism decreases, and therefore, the mechanism takes place at a much higher temperature.

Figure 2 displays marked places of the temperatures where the highest rate of phase transitions for precipitation and martensite reversion takes place. It should be noted that for higher applied in experiment heating rates, the time available for precipitation is decreasing influencing to a smaller specimen shrinkage. It is attributable to the low quantity of precipitates generated during heating at higher heating rates [13, 14]. However, it must be noted that this kind of material has a tendency to the segregation of alloying elements so the shrinkage can be different for different heating rates.

Phase transformations can occur by a number of mechanisms such as a shear process, a short-range diffusion process like a shuffle of atoms, or a diffusion-controlled

nucleation and growth process. The driving force (thermodynamics) and the time available (kinetics) decide the transformation process. In general, a diffusion-controlled nucleation and growth transformation is affected by the heating rate, and a shear or shuffle transformation is not. In addition, Fig. 2 leads to the conclusion that the austenite transition separates in two stages, i.e. in the first state through diffusion and the second stage through shear for lower heating rates and one stage through diffusion for higher heating rates. On the other hand, the beginning of martensite transform at lower heating rates to austenite takes place by shear process. At higher heating rates, the thermodynamic driving forces take over; therefore, transformation to austenite the residual martensite takes place by the diffusion mechanism. Because at higher heating rates, there is unsatisfactory time for shear occurring, consequently the whole martensite is changing to austenite by a single-stage diffusion mechanism. It is also capable to recognise that as the heating rate rises, the scale of precipitation reduces. This result means that precipitation in 300-grade maraging steel is primarily diffusion controlled.

Viswanathan et al. [24] reported that activation energies of transitions, estimated by the Kissinger method [14], may be expressed easier to understand the form:

$$\ln\left(\frac{T_M^2}{\Phi}\right) = \ln\left(\frac{E}{R}\right) - \ln(A) + \frac{E}{RT_M} \quad (1)$$

where  $\Phi$  is the heating rate,  $E$  is activation energy,  $R$  the universal gas constant, and  $T_M$  is the temperature at maximum phase transition rate. The mentioned equation is applicable only for a maximum transition rate. The kinetic parameter as expressed by activation energy for the reaction may be calculated from the slope of the straight line received by plotting  $T_M^2/\Phi$  on a logarithmic scale in relation to the reciprocity of  $T_M$ .

Figures 3 and 4 show the linear regression determined for the estimation the activation energies for precipitation of intermetallic phases and reversion of martensite applying the Kissinger equation, and Table 2 presents summarised activation energies ( $E$ ) estimated based on the slope of linear

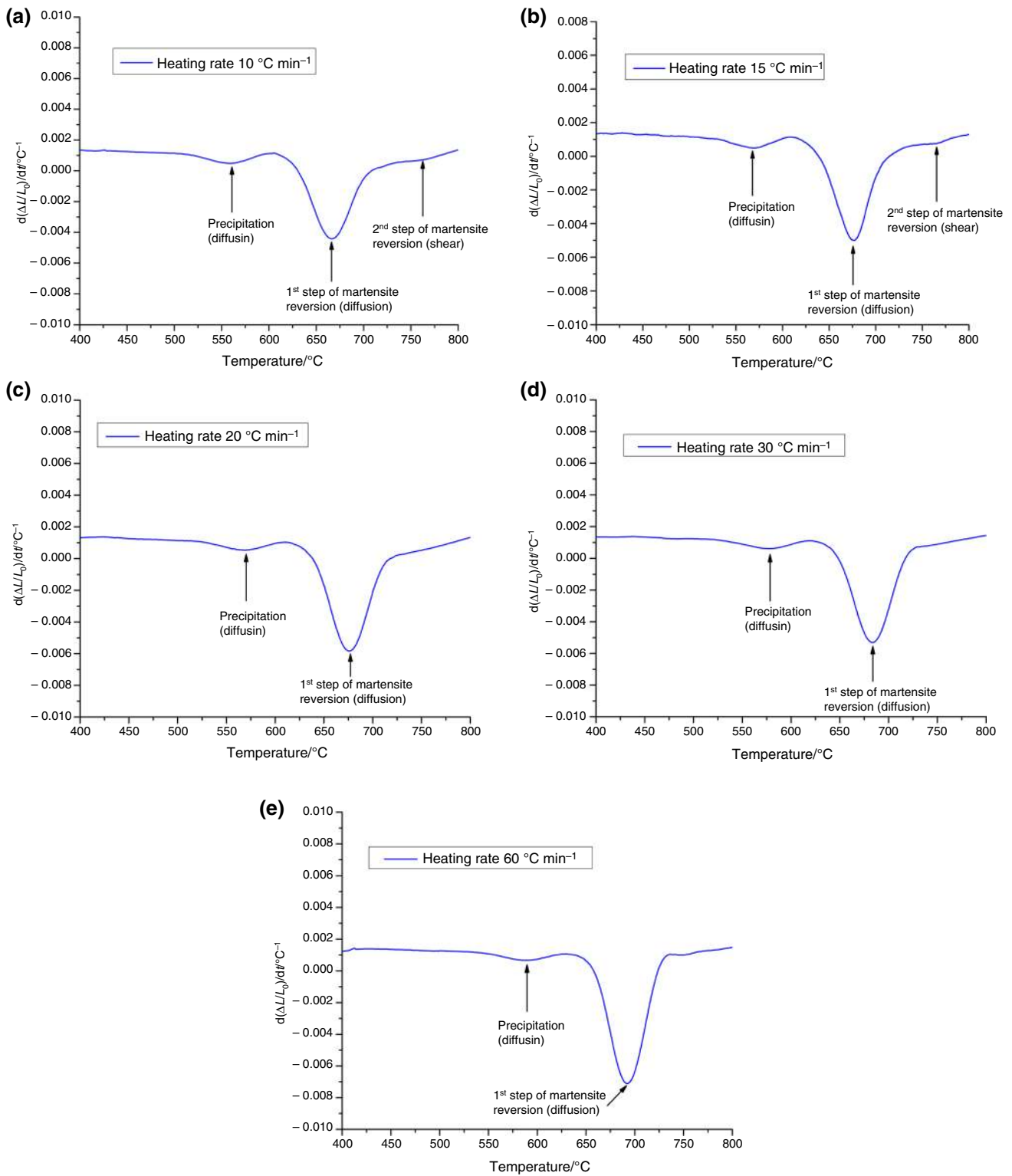


**Fig. 2** Variation of  $dL/dt$  of samples at **a**  $10\text{ }^{\circ}\text{C min}^{-1}$ ; **b**  $15\text{ }^{\circ}\text{C min}^{-1}$ ; **c**  $20\text{ }^{\circ}\text{C min}^{-1}$ ; **d**  $30\text{ }^{\circ}\text{C min}^{-1}$ ; **e**  $60\text{ }^{\circ}\text{C min}^{-1}$  SLM samples as a function of temperature

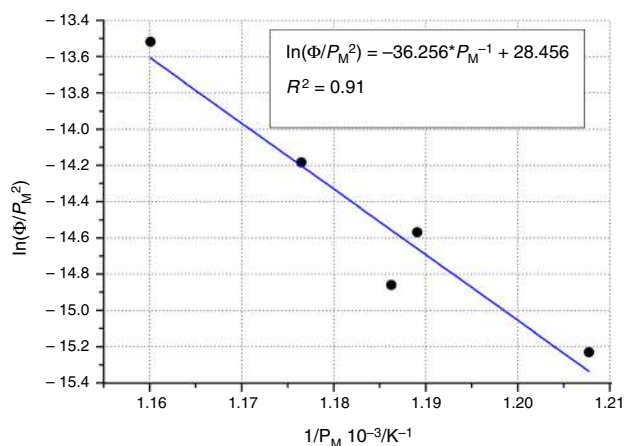


**Fig. 3** Linear regression determined for the evaluation of the activation energies for precipitation ( $P_M$ —temperature at maximum precipitation of intermetallic rate)

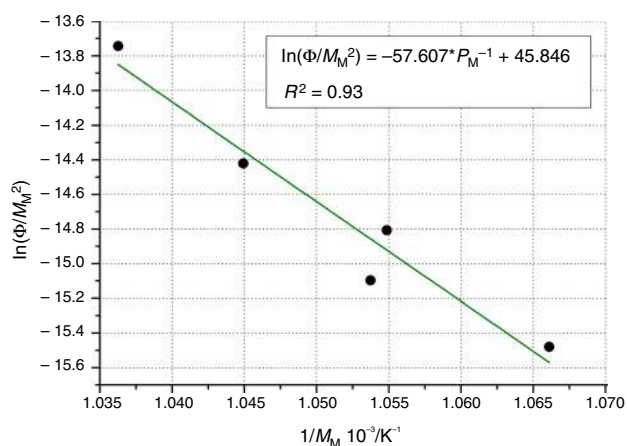


**Fig. 4** Linear regression determined for the estimation of the activation energies for reversion of martensite to austenite ( $M_M$ —temperature at maximum martensite reversion rate)

regression in relation to the results reported by other scientists [3, 13, 14, 24].

The as-built specimens may contain a large number of crystal defects, such as cell boundaries and dislocations developed through rapid solidification that occurs during SLM in a range  $10^3 \div 10^8 \text{ K s}^{-1}$  [29]. Certain defects react as preferential paths for atom migration, accelerating the diffusion-controlled precipitation mechanism. Some scientists discovered comparable activation energy values for strengthening precipitates formation in maraging steels manufactured through the traditional way. The activation energy for precipitation notified by Carvalho et al. [14] was  $272 \text{ kJ mol}^{-1}$  in the case of 300-grade maraging steel, while Viswanathan [24] reported a value of  $145 \text{ kJ mol}^{-1}$  in a 350-grade maraging steel. Guo et al. [3] acquired values of  $205 \text{ kJ mol}^{-1}$  in relation to a 250-grade maraging steel, while Kapoor et al. [13] gained a value of  $265 \text{ kJ mol}^{-1}$  in a 350-grade maraging steel.

Activation energy values for martensite reversion of  $562 \text{ kJ mol}^{-1}$  and of  $224 \text{ kJ mol}^{-1}$  were reported by Carvalho et al. and Viswanathan et al. and [14, 24], while  $342 \text{ kJ mol}^{-1}$  and  $423 \text{ kJ mol}^{-1}$  for  $\Phi < 2 \text{ }^\circ\text{C s}^{-1}$  and  $828 \text{ kJ mol}^{-1}$   $\Phi > 2 \text{ }^\circ\text{C s}^{-1}$  were reported by Guo et al. and Kapoor et al. [3, 13].

Besides, Table 3 indicates that there is a variance in the activation energy values of the precipitation of intermetallic phases as a function of the heating rate. It can be noted that the lattice diffusion mechanism is dominant for lower heating rates, since the activation energy ( $301 \text{ kJ mol}^{-1}$ ) is near to those of titanium ( $272 \text{ kJ mol}^{-1}$ ), nickel ( $246 \text{ kJ mol}^{-1}$ ) and molybdenum ( $238 \text{ kJ mol}^{-1}$ ). (In ferrite, the mechanism is diffusion.) It also can be observed that there is a variance in the activation energy of martensite reversion as a function of the heating rate. In work [13] for higher heating rates, propose that for  $\Phi < 2 \text{ }^\circ\text{C s}^{-1}$ , activation energy of martensite reversion is  $423 \text{ kJ mol}^{-1}$  and for  $\Phi > 2 \text{ }^\circ\text{C s}^{-1}$  activation energy is  $828 \text{ kJ mol}^{-1}$ . The research has revealed that activation energy is more massive due to the shear mechanism that takes place more expressively. In the presented work, analysis was carried out on similar material, however, manufactured in a non-conventional way such as selective laser melting technique

**Table 3** Precipitation of intermetallic phases and martensite reversion activation energies for different grades of maraging steels

	References				
	SLM (maraging 300)	Carvalho et al. (maraging 300)	Viswanathan et al. (maraging 300)	Guo et al. (maraging 250)	Kapoor et al. (maraging 350)
Heating rate	$10 \div 60/^\circ\text{C min}^{-1}$	$1 \div 28/^\circ\text{C s}^{-1}$	$10 \div 40/^\circ\text{C min}^{-1}$	$5 \div 50/^\circ\text{C min}^{-1}$	$0.2 \div 200/^\circ\text{C s}^{-1}$
Precipitation ( $\text{kJ mol}^{-1}$ )	301	$272 \pm 18$	$145 \pm 4$	205	265
Martensite reversion ( $\text{kJ mol}^{-1}$ )	478	$562 \pm 69$	$224 \pm 4$	342	$423; \Phi < 2/^\circ\text{C s}^{-1}$ $828; \Phi > 2/^\circ\text{C s}^{-1}$

and showed that the shearing mechanism also takes place with larger intensity for higher heating rates.

## Conclusions

A non-isothermal dilatometric technique with different heating rates of 10, 15, 20, 30 and 60 °C min<sup>-1</sup> was applied to analyse the kinetics of solid-state transitions in an 18-Ni 300-grade maraging steel manufactured by selective laser technique. The results are summarised as follows:

- The martensite reversion to austenite transition in analysed compounds discloses a trend to split into two stages for low heating rates. The first stage of these transitions, become by a low heating rate, occurs within a lattice diffusion mechanism, while the second stage, enhanced by a high heating rate, takes place within a shear mechanism.
- The activation energy of 301 kJ mol<sup>-1</sup> was found out for the precipitation of intermetallic phases. For the reversion of martensite to austenite, the activation energy of 478 kJ mol<sup>-1</sup> was found.
- The non-isothermal dilatometric method can be taken into consideration as a uncomplicated substitute for labour-intensive and time-consuming isothermal hardness analysis.

**Acknowledgements** The results in this publication were obtained as part of the research co-financed by the rector's grant in the area of scientific research and development works, Silesian University of Technology, 10/010/RGJ19/0269. Work has been done in connection with project Innovative and additive manufacturing technology—new technological solutions for 3D printing of metals and composite materials, Reg. No. CZ.02.1.01/0.0/0.0/17\_049/0008407 financed by Structural Funds of Europe Union.

**Open Access** This article is licensed under a Creative Commons Attribution 4.0 International License, which permits use, sharing, adaptation, distribution and reproduction in any medium or format, as long as you give appropriate credit to the original author(s) and the source, provide a link to the Creative Commons licence, and indicate if changes were made. The images or other third party material in this article are included in the article's Creative Commons licence, unless indicated otherwise in a credit line to the material. If material is not included in the article's Creative Commons licence and your intended use is not permitted by statutory regulation or exceeds the permitted use, you will need to obtain permission directly from the copyright holder. To view a copy of this licence, visit <http://creativecommons.org/licenses/by/4.0/>.

## References

1. Mouritz AP. Introduction to aerospace materials. Cambridge: Woodhead Publishing; 2012.
2. Turk C, Zunko H, Aumayr C, Leitner H, Kapp M. Advances in maraging steels for additive manufacturing. *Berg Huettenmaenn Monatsh.* 2019;164(3):112–6.
3. Sha W, Guo Z. Maraging steels: modelling of microstructure properties and applications. Cambridge: Woodhead Publishing Limited; 2009.
4. Sroka M, Zieliński A, Mikuła M. The service life of the repair welded joint of Cr–Mo/Cr–Mo–V. *Arch Metall Mater.* 2016;61(3):969–74.
5. Bhardwaj T, Shukla M. Effect of laser scanning strategies on texture, physical and mechanical properties of laser sintered maraging steel. *Mater Sci Eng A Struct.* 2018;734:102–9.
6. Pereloma EV, Shekhter A, Miller MK, Ringer SP. Ageing behaviour of an Fe–20Ni–1.8Mn–1.6Ti–0.59Al (wt%) maraging alloy: clustering, precipitation and hardening. *Acta Mater.* 2004;52(19):5589–602.
7. Ahmed M, Nasim I, Husain SW. Influence of nickel and molybdenum on the phase stability and mechanical properties of maraging steels. *J Mater Eng Perform.* 1994;3(2):248–54.
8. Li X, Yin Z. Reverted austenite during aging in 18Ni (350) maraging steel. *Mater Lett.* 1995;24(4):239–42.
9. Peters DT. A Study of austenite reversion during aging of maraging steels. *Trans. ASM.* 1968;61:62–74.
10. Tavares SSM, Abreu HFG, Maria Neto J, Da Silva MR, Popa I. A thermomagnetic study of the martensite-austenite transition in the maraging 350 steel. *J Alloy Compd.* 2003;358:153–6.
11. Tavares SSM, Da Silva MR, Maria Neto J, Pardal JM, Cindra Fonseca MP. Magnetic properties of a Ni–Co–Mo–Ti maraging 350 steel. *J Alloy Compd.* 2004;373:304–11.
12. Viswanathan UK, Dey G, Sethumandhavan V. Effects of austenite reversion during overageing on the mechanical properties of 18Ni (350) maraging steel. *Mater Sci Eng.* 2005;398:367–72.
13. Kapoor R, Kumar L, Batra IS. A dilatometric study of the continuous heating transformations in 18 wt% Ni maraging steel of grade 350. *Mater Sci Eng A Struct.* 2003;352:318–24.
14. Carvalho LG, Andrade MS, Plaut RL, Souza FM, Padilha AF. A dilatometric study of the phase transformations in 300 and 350 maraging steels during continuous heating rates. *Mater Res.* 2013;16(4):740–4.
15. Reis AG, Reis DAP, Abdalla AJ, Otubo J, Sandim HRZ. A dilatometric study of the continuous heating transformations in maraging 300 steel. *IOP Conf Ser Mater Sci Eng.* 2015;97:1–4.
16. Pektaş I, Atala H. The effects of various heat treating parameters on the hardness and microstructures of the experimental 18% nickel maraging steels. *J Therm Anal Calorim.* 1998;54(3):803–14.
17. Menapace C, Lonardelli I, Molinari A. Phase transformation in a nanostructured M300 maraging steel obtained by SPS of mechanically alloyed powders. *J Therm Anal Calorim.* 2010;101:815–21.
18. Snopiński P, Król M, Tański T, Krupinska B. Effect of cooling rate on microstructural development in alloy ALMG9. *J Therm Anal Calorim.* 2018;133:379–90.
19. Król M. Effect of grain refinements on the microstructure and thermal behaviour of Mg–Li–Al alloy. *J Therm Anal Calorim.* 2018;133:246.
20. Krupinski M, Labisz K, Tanski T, Krupinska B, Krol M, Polok-Rubiniec M. Influence of Mg addition on crystallisation kinetics and structure of the Zn–Al–Cu alloy. *Arch Metall Mater.* 2016;61(2):785–9.
21. Król M, Tański T, Matula G, Snopiński P, Tomiczek AE. Analysis of crystallisation process of cast magnesium alloys based on thermal derivative analysis. *Arch Metall Mater.* 2015;60(4):2993–9. <https://doi.org/10.1515/amm-2015-0478>.
22. Andrés CG, Caballero FG, Capdevilla C, Álvarez LF. Application of dilatometric analysis to the study of solid-solid phase transformations in steels. *Mater Charact.* 2002;48(1):101–11.
23. Oliveira FLG, Andrade MS, Cota AB. Kinetics of austenite formation during continuous heating in low carbon steel. *Mater Charact.* 2007;58(3):256–61.

24. Viswanathan UK, Kuttly TRG, Ganguly C. Dilatometric technique for evaluation of the kinetics of solid-state transformation of maraging steel. *Metall Trans A*. 1993;24(12):2653–6.
25. Sroka M, Nabiałek M, Szota M, Zieliński A. The influence of the temperature and ageing time on the NiCr<sub>23</sub>Co<sub>12</sub>Mo alloy microstructure. *Rev Chim-Bucharest*. 2017;4:737–41.
26. Zaeh MF, Branner G. Investigations on residual stresses and deformations in selective laser melting. *Prod Eng*. 2010;4(1):35–45.
27. Casalino G, Campanelli SL, Contuzzi N, Ludovico AD. Experimental investigation and statistical optimisation of the selective laser melting process of a maraging steel. *Opt Laser Technol*. 2015;65:151–8.
28. Krol M, Tanski T. Surface quality research for selective laser melting of Ti–6Al–4V Alloy. *Arch Metall Mater*. 2016;61(3):945–50.
29. Casati R, Lemke J, Vedani M. Microstructural and mechanical properties of as built, solution treated and aged 18 Ni (300 grade) maraging steel produced by selective laser melting. *La Metall Ital*. 2017;1:11–20.

**Publisher's Note** Springer Nature remains neutral with regard to jurisdictional claims in published maps and institutional affiliations.